

**METHOD OF DIMENSIONALITY REDUCTION IN CONTACT
MECHANICS AND FRICTION: A USERS HANDBOOK.
I. AXIALLY-SYMMETRIC CONTACTS**

UDC (539.3)

Valentin L. Popov, Markus Hess

Technical University Berlin

Abstract. *The Method of Dimensionality Reduction (MDR) is a method of calculation and simulation of contacts of elastic and viscoelastic bodies. It consists essentially of two simple steps: (a) substitution of the three-dimensional continuum by a uniquely defined one-dimensional linearly elastic or viscoelastic foundation (Winkler foundation) and (b) transformation of the three-dimensional profile of the contacting bodies by means of the MDR-transformation. As soon as these two steps are completed, the contact problem can be considered to be solved. For axial symmetric contacts, only a small calculation by hand is required which does not exceed elementary calculus and will not be a barrier for any practically-oriented engineer. Alternatively, the MDR can be implemented numerically, which is almost trivial due to the independence of the foundation elements. In spite of their simplicity, all the results are exact. The present paper is a short practical guide to the MDR.*

Key Words: *Normal Contact, Tangential Contact, Adhesion, Friction, Partial Slip, Stress*

1. INTRODUCTION

In the recently published book [1], the so-called method of dimensionality reduction (MDR) is described for the first time in detail. MDR can be traced back to the solution of the normal contact problem by Galin (Russian Academy of Sciences) in the 1940s [2]. His results were later published by Sneddon and, in this way, made public to the western world [3]. The method of dimensionality reduction takes these results and puts them into such a form that even a layman in the field of contact mechanics can use them for a multitude of contact mechanical problems. In doing this, it merges the ideas and results from Cattaneo [4], Mindlin [5], Jaeger [6], and Ciavarella [7] about a close relationship between normal and tangential contacts, the solutions of Galanov and Borodich [8, 9, 10]

Received February 20, 2014

Corresponding author: Valentin Popov

TU Berlin, Department of System Dynamics and Physics of Friction, Berlin, Germany

E-mail: v.popov@tu-berlin.de

for adhesive contacts of axially-symmetric profiles of power functions (later found independently by Yao and Gao [11]), as well as the theory of Lee and Radok about the relationship between elastic and viscoelastic contacts [12, 13].

The book [1] contains all of the necessary evidence and many examples of how to apply the MDR. However, it has proven to be too comprehensive for practical users. There is a need for the fundamental ideas and "recipes" of the MDR to be presented in a concise way without extensive reasoning or proof, a sort of "user's handbook." This work is dedicated to exactly such a practical instruction for the method of dimensionality reduction.

2. TWO INTRODUCTORY STEPS OF THE MDR

We consider a contact between two elastic bodies with moduli of elasticity of E_1 and E_2 , Poisson's numbers of ν_1 and ν_2 , and shear moduli of G_1 and G_2 , accordingly. In this work, we restrict ourselves to the axially-symmetric profiles, which is not necessarily required. A generalization to profiles that are not axially-symmetric is possible, but is not considered in this work. We denote the difference between the profiles of bodies as $z = f(r)$. In the framework of the MDR, two independent steps are conducted:

The first step: First, the three-dimensional elastic (or viscoelastic) bodies are replaced by a one-dimensional linearly elastic foundation. This is considered to be a linear array of elements having independent degrees of freedom and a sufficiently small separation distance Δx , Fig. 1.

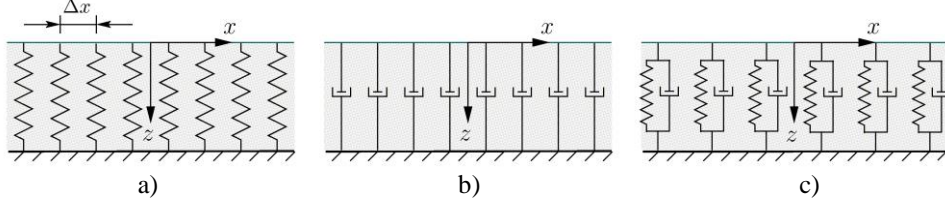


Fig. 1 One-dimensional foundation of different materials: elastic foundation (a), purely viscous foundation (b), and viscoelastic foundation (c) with an example rheology according to Kelvin-Voigt

In the simplest case of the elastic contact, the foundation consists of linearly elastic spring elements that have normal stiffness Δk_z and tangential stiffness Δk_x (Fig. 1a):

$$\Delta k_z = E^* \Delta x \quad \text{with} \quad \frac{1}{E^*} = \frac{1-\nu_1^2}{E_1} + \frac{1-\nu_2^2}{E_2}, \quad (1)$$

$$\Delta k_x = G^* \Delta x \quad \text{with} \quad \frac{1}{G^*} = \frac{2-\nu_1}{4G_1} + \frac{2-\nu_2}{4G_2}. \quad (2)$$

Starred values E^* and G^* denote the effective elastic moduli. Incompressible linearly viscous materials are presented by a linear damping element with damping coefficient $\Delta \gamma$ (Fig. 1b), which is dependent on the viscosity η of the viscoelastic partner according to:

$$\Delta\gamma = 4\eta\Delta x. \quad (3)$$

Arbitrary combinations of these two base elements are also possible in order to satisfy the most complicated elastomers – Fig. 1c, for example, shows a viscoelastic foundation built out of elements of in parallel connected springs and dampers (Kelvin-Voigt model). In this paper, we will restrict ourselves to the case of "elastically similar" materials:

$$\frac{1-2\nu_1}{G_1} = \frac{1-2\nu_2}{G_2}, \quad (4)$$

which guarantees the independence of the normal and tangential contact problems [14]. This condition is always met in important cases of contacts between the bodies with the same elastic properties or those between a rigid body and an elastomer.

The second step: In the second step, three-dimensional profile $z = f(r)$ (Fig. 2, left) is transformed into a one-dimensional profile (Fig. 2, right) according to:

$$g(x) = |x| \int_0^{|x|} \frac{f'(r)}{\sqrt{x^2 - r^2}} dr. \quad (5)$$

The reverse transformation is:

$$f(r) = \frac{2}{\pi} \int_0^r \frac{g(x)}{\sqrt{r^2 - x^2}} dx. \quad (6)$$

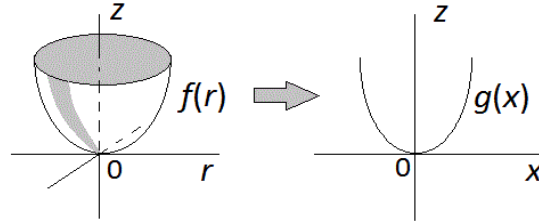


Fig. 2 The three-dimensional profile is transformed into a one-dimensional profile using the MDR

For a less trivial example, we consider the contact of a *parabolic profile with a worn tip* (Fig. 3):

$$f(r) = \begin{cases} 0 & \text{for } 0 \leq r \leq b \\ \frac{r^2 - b^2}{2R} & \text{for } b \leq r \leq a \end{cases}. \quad (7)$$

The MDR transformed profile according to Eq. (5) is given by:

$$g(x) = \begin{cases} 0 & \text{for } 0 \leq |x| \leq b \\ \frac{|x|}{R} \sqrt{x^2 - b^2} & \text{for } b \leq |x| \leq a \end{cases}. \quad (8)$$

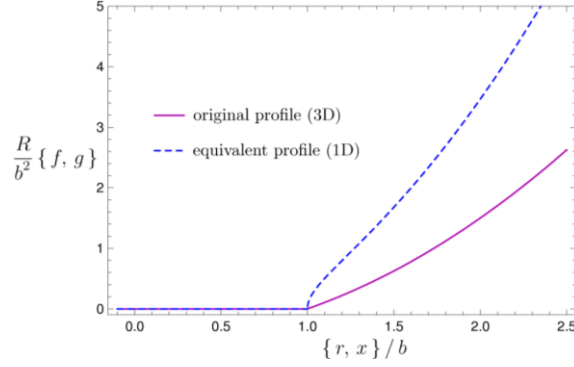


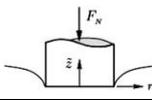
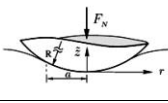
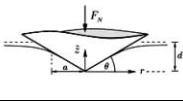
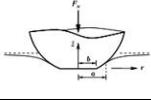
Fig. 3 Parabolic indenter with a "worn" tip: original (solid line) and equivalent (dashed line) profiles for comparison

Examples for the MDR transformation

By inserting profiles into Eq. (5) that correspond to a cylinder, paraboloid, cone, or an arbitrary power function $z \sim r^n$, we obtain the MDR transformed one-dimensional profiles which are summarized in Table 1, where:

$$k_n = \frac{\sqrt{\pi}}{2} \frac{n\Gamma\left(\frac{n}{2}\right)}{\Gamma\left(\frac{n}{2} + \frac{1}{2}\right)} \quad \text{and} \quad \Gamma(n) := \int_0^{\infty} t^{n-1} e^{-t} dt \text{ is the gamma function.}$$

Table 1 The three-dimensional profile is transformed into a one-dimensional profile using the MDR

				arbitrary n	
$f(r)$	$\begin{cases} 0, & r < a \\ \infty, & r > a \end{cases}$	$r^2 / 2R$	$r \tan \theta$	$c_n r^n$	Eq. (7)
$g(x)$	$\begin{cases} 0, & x < a \\ \infty, & x > a \end{cases}$	x^2 / R	$\frac{\pi}{2} x \tan \theta$	$\kappa_n c_n x ^n$	Eq. (8)

3. CALCULATION STEP OF THE MDR USING THE EXAMPLE OF A NORMAL CONTACT WITHOUT ADHESION

The one-dimensional profile according to Eq. (5) is now pressed into an elastic foundation corresponding to Eq. (1) with normal force F_N (see Fig. 4). The normal surface displacement at point x within the contact area results from the difference between indentation depth d and profile form g :

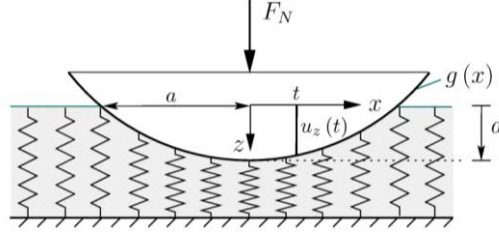


Fig. 4 Equivalent model for a Hertzian contact

$$u_z(x) = d - g(x). \quad (9)$$

At the edge of non-adhesive contact $x = \pm a$, the surface displacement must be zero:

$$u_z(\pm a) = 0 \Rightarrow d := g(a). \quad (10)$$

This equation determines the relationship between the indentation depth and contact radius a . It should be noted that this relationship is independent of the rheology of the medium. The force of a spring at the point x is proportional to the displacement at this point:

$$\Delta F_z(x) = \Delta k_z u_z(x) = E^* u_z(x) \Delta x, \quad (11)$$

and the sum of all spring forces must correspond to the normal force in equilibrium. In the limiting case of very small spring separation distances $\Delta x \rightarrow dx$, the summation becomes the integral:

$$F_N := E^* \int_{-a}^a u_z(x) dx = 2E^* \int_0^a (d - g(x)) dx. \quad (12)$$

Equation (12) provides the normal force in dependence on the contact radius and on the indentation depth, if Eq. (10) is taken into account.

We now define linear force density $q_z(x)$:

$$q_z(x) := \frac{\Delta F_z(x)}{\Delta x} = E^* u_z(x). \quad (13)$$

The stress distribution in the original three-dimensional system can be determined with the help of the one-dimensional distributed load using the integral transformation [15]:

$$p(r) = -\frac{1}{\pi} \int_r^\infty \frac{q'(x)}{\sqrt{x^2 - r^2}} dx. \quad (14)$$

The normal surface displacement (both inside and outside of the contact area) is given by the transformation:

$$u_z(r) = \frac{2}{\pi} \int_0^r \frac{u_z(x)}{\sqrt{r^2 - x^2}} dx. \quad (15)$$

We point out once more that one-dimensional values contain the independent variable x , while three-dimensional values contain radial variable r ; function $u_z(x)$ inside the integrand of Eq. (15) means the surface displacement of the linearly elastic foundation. We will carry out the last two transformations using the example of a cone. The three-dimensional profile in this case is $f(r) = r \cdot \tan \theta$; the MDR transformed profile is $g(x) = \frac{\pi}{2} |x| \tan \theta$. The displacement within the contact area is $u_z(x) = d - \frac{\pi}{2} |x| \tan \theta$. The linear force density is $q(x) = E^* \left(d - \frac{\pi}{2} |x| \tan \theta \right)$ and its derivative is $q'(x) = -\frac{\pi}{2} E^* \tan \theta$ (for positive x). Insertion into Eq. (14) and Eq. (15) results in:

$$p(r) = \frac{E^*}{2} \tan \theta \int_r^a \frac{dx}{\sqrt{x^2 - r^2}} = \frac{E^*}{2} \tan \theta \cdot \ln \left(\frac{a}{r} + \sqrt{\left(\frac{a}{r}\right)^2 - 1} \right), \quad (16)$$

$$u_z(r) = \frac{2}{\pi} \int_0^a \frac{d - (\pi/2)x \tan \theta}{\sqrt{r^2 - x^2}} dx = \frac{2d}{\pi} \left[\arcsin \left(\frac{a}{r} \right) - \left(\frac{r}{a} - \sqrt{\left(\frac{r}{a}\right)^2 - 1} \right) \right]. \quad (17)$$

Equation (17) gives the normal surface displacement outside of the contact area. A similar calculation for a parabolic profile $f(r) = r^2/(2R)$ initially provides $u_z(x) = d - x^2/R$ and, after insertion into Eq. (15), results in:

$$u_z(r) = \frac{d}{\pi} \left[\left(2 - \left(\frac{r}{a}\right)^2 \right) \cdot \arcsin \left(\frac{a}{r} \right) + \sqrt{\left(\frac{r}{a}\right)^2 - 1} \right]. \quad (18)$$

For the contact of a flattened paraboloid, Eq. (7), we obtain the contact radius by using Eq. (10):

$$u_z(a) = 0 \Rightarrow d := g(a) = \frac{a}{R} \sqrt{a^2 - b^2}. \quad (19)$$

and the normal force using Eq.(12):

$$F_N = 2E^* \int_0^a d dx - \frac{2E^*}{R} \int_0^a x \sqrt{x^2 - b^2} dx = \frac{2E^*}{3R} (2a^2 + b^2) \cdot \sqrt{a^2 - b^2}. \quad (20)$$

These results correspond of course with those of Eijke [18] from the three-dimensional theory.

Examples for normal contacts

Insertion of the MDR transformed profiles into Eqs. (10) and (12) and an elementary integration provides the results for the "classical profiles" of a cylinder [17], sphere [16], and cone [3] as well as the general power profile [2], which are summarized in Table 2. The order of the rows corresponds to the order of the calculation steps.

Table 2 Solutions to the normal contact problem for simple profiles

3D profile $f(r)$	$\begin{cases} 0, & r < a \\ \infty, & r > a \end{cases}$	$r^2 / 2R$	$r \tan \theta$	$c_n r^n$
1D profile $g(x)$	$\begin{cases} 0, & x < a \\ \infty, & x > a \end{cases}$	x^2 / R	$\frac{\pi}{2} x \tan \theta$	$\kappa_n c_n x ^n$
contact radius a , according to (10)	a	\sqrt{Rd}	$\frac{2}{\pi} \frac{d}{\tan \theta}$	$\left(\frac{d}{\kappa_n c_n} \right)^{1/n}$
normal force F_N , according to (12)	$2aE^*d$	$\frac{4}{3} E^* R^{1/2} d^{3/2}$	$\frac{2}{\pi} E^* \frac{d^2}{\tan \theta}$	$\frac{2n}{n+1} \frac{E^* d^{n+1}}{(c_n \kappa_n)^{1/n}}$
stress distribution $p(r)$, according to (14)	$\frac{E^* d}{\pi a} \frac{1}{\sqrt{1 - \left(\frac{r}{a}\right)^2}}$	$\frac{2E^*}{\pi} \left(\frac{d}{R}\right)^{1/2} \sqrt{1 - \left(\frac{r}{a}\right)^2}$	Eq. (16)	
displacement $u_z(r)$ according to (15) for $r > a$	$\frac{2d}{\pi} \arcsin\left(\frac{a}{r}\right)$	Eq. (18)	Eq. (17)	

4. ADHESIVE NORMAL CONTACT

The MDR rule for the mapping of adhesive contacts will be formulated in the following. As with the non-adhesive contact, the MDR transformed one-dimensional profile is brought into contact with the linearly elastic foundation defined in Section 2. Now, it will be assumed that all of the springs in the contact adhere to the indenter, then the contact radius remains the same after a successive decrease in the normal force. From the edge of the contact towards the middle, however, more and more springs will be loaded in tension. As soon as the change in length of the outer springs reaches the maximum allowable value:

$$\Delta l(\pm a) = \Delta l_{\max}(a) := \sqrt{\frac{2\pi a \Delta \gamma}{E^*}}, \quad (21)$$

there will be a state of indifference between adhesion and separation (Fig. 5). Here, $\Delta \gamma$ is the separation energy of the contacting bodies per unit area. This state corresponds exactly to the equilibrium state of the three-dimensional adhesive contact [15].

In contrast to the algorithm for non-adhesive contact, Equation (10) must only be replaced by:

$$u_z(\pm a) = -\Delta l_{\max}(a) \Rightarrow d := g(a) - \Delta l_{\max}(a) \quad (22)$$

in order to calculate the indentation depth. The normal force is given as before by Eq. (12):

$$F_N = 2E^* \int_0^a (d - g(x)) dx = 2E^* \left[ad - \int_0^a g(x) dx \right] = 2E^* \left[ag(a) - \int_0^a g(x) dx - a \Delta l_{\max}(a) \right] \quad (23)$$

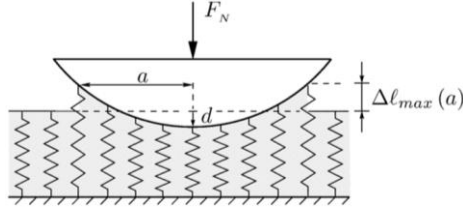


Fig. 5 Illustration for the MDR rule for an adhesive contact

or

$$F_N = 2E^* \left[\int_0^a xg'(x)dx - a\Delta l_{\max}(a) \right]. \quad (24)$$

If the force is controlled during the separation, then critical value a_c of the contact radius at the moment of the loss of stability is determined by condition $dF_N/da = 0$:

$$\frac{dg(a)}{da} = \sqrt{\frac{9\pi\Delta\gamma}{2aE^*}}. \quad (25)$$

Inserting the critical radius obtained from this equation into Eq. (23) results in the maximum negative force. We will call its magnitude the adhesion force F_A :

$$F_A = 2E^* \left[a_c \Delta l_{\max}(a_c) - \int_0^{a_c} xg'(x)dx \right]. \quad (26)$$

The simplest example is calculating the adhesion force between a cylinder with the radius a and an elastic half-space. In this case, the integral in Eq. (26) is equal to zero and the adhesion force is only given by the first term: $F_A = 2E^* a \Delta l_{\max}(a) = \sqrt{8\pi a^3 E^* \Delta\gamma}$, which corresponds to the result of Kendall [20]. Calculations for other profiles are just as simple and are summarized in Table 3.

In order to stress the generality and simplicity of the calculation method, we will now conduct the calculation for a *parabolic profile with a worn tip* (Fig. 6). If we take the equivalent profile from Equation (8) into account, the resulting indentation depth is:

$$d(a) := g(a) - \Delta l_{\max}(a) = \frac{a}{R} \sqrt{a^2 - b^2} - \sqrt{\frac{2\pi a \Delta\gamma}{E^*}}, \quad (27)$$

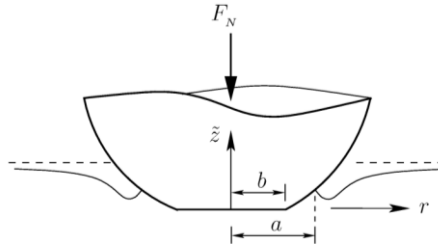


Fig. 6 Qualitative presentation of the adhesive contact of a parabolic profile with a flattened tip

and from Eq. (12), the normal force is:

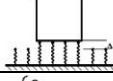
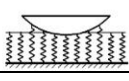
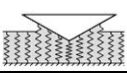
$$F_N(a) = E^* \int_{-a}^a u_z(x) dx = \frac{2E^*}{3R} (2a^2 + b^2) \sqrt{a^2 - b^2} - \sqrt{8\pi a^3 E^* \Delta\gamma}. \quad (28)$$

This equation corresponds to the results from the three-dimensional theory [22].

Examples for adhesive normal contacts

Inserting the MDR transformed profiles into Eqs. (25) and (26) and conducting an elementary integration provides the results summarized in Table 3 for the "classical profiles" of the cylinder [20], sphere [19], and cone [21], as well as the general power function profile [10, 11]. The order of the rows corresponds to the order of the calculation steps.

Table 3 Solutions for adhesive contacts for simple profiles

				arbitrary n
3D profile $f(r)$	$\begin{cases} 0, & r < a \\ \infty, & r > a \end{cases}$	$r^2 / 2R$	$r \tan \theta$	$c_n r^n$
1D profile $g(x)$	$\begin{cases} 0, & x < a \\ \infty, & x > a \end{cases}$	x^2 / R	$\frac{\pi}{2} x \tan \theta$	$\kappa_n c_n x ^n$
critical contact radius a_c , according to (25)	a	$\left(\frac{9\pi\Delta\gamma R^2}{8E^*} \right)^{1/3}$	$\frac{18\Delta\gamma}{\pi E^* \tan^2 \theta}$	$\left(\frac{9\pi\Delta\gamma}{2E^* n^2 \kappa_n^2 c_n^2} \right)^{1/3}$
Adhesive force F_A , according to (26)	$\sqrt{8\pi a^3 E^* \Delta\gamma}$	$\frac{3}{2} \pi \Delta\gamma R$	$\frac{54\Delta\gamma^2}{\pi \tan^3 \theta \cdot E^*}$	$\frac{2n-1}{n+1} \left[\left(\frac{3}{2n\kappa_n c_n} \right)^3 (2\pi\Delta\gamma)^{n+1} E^{*n-2} \right]^{\frac{1}{2n-1}}$

5. TANGENTIAL CONTACT

We now consider an axially-symmetric indenter that is initially pressed into an elastic half-space with normal force F_N and subsequently loaded with tangential force F_x in the x -direction (Fig. 7). We assume that Coulomb's law of friction is valid in the simplest

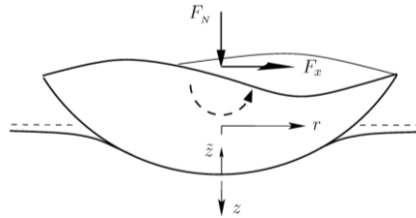


Fig. 7 Qualitative presentation of the tangential contact

form in the contact: as long as tangential stress τ is smaller than the coefficient of friction μ times normal stress p , the surface is in a state of sticking. After slip sets in, the tangential stress remains constant and equal to μp :

$$\tau(r) \leq \mu p(r) \text{ for stick,} \quad (29)$$

$$\tau(r) = \mu p(r) \text{ for slip.} \quad (30)$$

It is known that for a small tangential force at the edge of the contact, a ring-shaped slip domain develops, which expands inwards for increasing force until the complete slip is exhibited. We denote the inner radius of the slip domain (or the radius of the stick domain) with c .

The MDR is applied to the tangential contact as follows. The modified profile $g(x)$ is pressed into the linearly elastic foundation with force F_N and then tangentially displaced by $u_x^{(0)}$. The linearly elastic foundation is denoted by the stiffnesses according to (1) and (2). Every spring sticks to the indenter and is displaced along with it as long as the tangential force $\Delta F_x = k_x u_x^{(0)}$ is smaller than $\mu \Delta F_z$. After the adhesion force is reached, the spring begins to slip and the force remains constant and equal to $\mu \Delta F_z$. This rule can also be incrementally formulated so that it can be applied for arbitrary loading histories: for a small displacement of indenter of $\Delta u_x^{(0)}$, we obtain:

$$\begin{aligned} \Delta u_x(x) &= \Delta u_x^{(0)}, & \text{if } |k_x u_x(x)| < \mu f_z \\ u_x(x) &= \pm \frac{\mu \Delta F_z(x)}{k_x}, & \text{in a state of slip} \end{aligned} \quad (31)$$

The sign of the last equation is dependent on the direction of motion of the indenter. By following the incremental changes in the position of the indenter, we can explicitly determine the displacement of all the springs in the contact area; with this, all tangential forces:

$$\Delta F_x = k_x u_x(x) = G^* \Delta x \cdot u_x(x). \quad (32)$$

and the linear force density (distributed load):

$$q_x(x) = \frac{\Delta F_x}{\Delta x} = G^* u_x(x) \quad (33)$$

are also known. The distribution of tangential stress $\tau(r)$ as well as displacements $u_x(r)$ in the original three-dimensional contact are determined as follows [1]:

$$u_x(r) = \frac{2}{\pi} \int_0^r \frac{u_x(x)}{\sqrt{r^2 - x^2}} dx. \quad (34)$$

$$\tau(r) = -\frac{1}{\pi} \int_r^\infty \frac{q'_x(x)}{\sqrt{x^2 - r^2}} dx = -\frac{G^*}{\pi} \int_r^\infty \frac{u'_x(x)}{\sqrt{x^2 - r^2}} dx. \quad (35)$$

If the indenter is displaced in one direction from the equilibrium position, then radius c of the stick domain is determined from the condition that tangential force $k_x u_x^{(0)}$ is equal to μ times normal force $k_z u_z(c)$ (Fig. 8):

$$G^* u_x^{(0)} = \mu E^* (d - g(c)). \quad (36)$$

The tangential displacement is equal to:

$$u_x(x) = \begin{cases} u_x^{(0)}, & \text{for } x < c \\ \mu \left(\frac{E^*}{G^*} \right) (d - g(x)), & \text{for } c < x < a \end{cases}, \quad (37)$$

the distributed load is:

$$q(x) = \begin{cases} G^* u_x^{(0)}, & \text{for } x < c \\ \mu E^* (d - g(x)), & \text{for } c < x < a \end{cases}, \quad (38)$$

and the resulting tangential force is²:

$$F_x = 2 \int_0^a q_x(x) dx = 2\mu E^* \left[c(d - g(c)) + \int_c^a (d - g(x)) dx \right]. \quad (39)$$

The normal force is still given by Equation (12) and ratio $F_x/(\mu F_N)$ is given by:

$$\frac{F_x}{\mu F_N} = \frac{\int_c^a x g'(x) dx}{ag(a) - \int_0^a g(x) dx}. \quad (40)$$

The relative displacement $\Delta u_x = u_x^{(0)} - u_x(x)$ of the surfaces in contact is obtained by subtracting $u_x^{(0)}$ from Eq. (37):

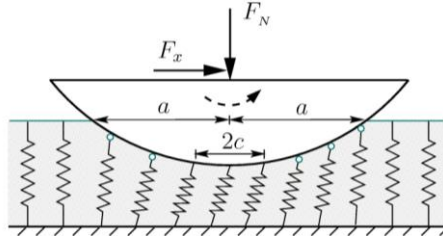


Fig. 8 Equivalent model for the classical tangential contact according to Cattaneo and Mindlin

$$\Delta u_x = \begin{cases} 0, & \text{for } x < c \\ \mu \left(\frac{E^*}{G^*} \right) (g(c) - g(x)), & \text{for } c < x < a \end{cases}. \quad (41)$$

² We stress once more that all macroscopic values obtained using the procedure described above correspond exactly to the three-dimensional solutions of Cattaneo [4], Mindlin [5], Jaeger [6] and Ciavarella [7].

The relative displacement in the original three-dimensional system is calculated using Eq. (34) as:

$$u_x(r) = \frac{2}{\pi} \mu \left(\frac{E^*}{G^*} \right) \int_0^r \frac{g(c) - g(x)}{\sqrt{r^2 - x^2}} dx, \quad \text{for } c < r < a. \quad (42)$$

For example, for a conical, we obtain:

$$u_x(r) = \mu \left(\frac{E^*}{G^*} \right) c \tan \theta \left[-\sqrt{\left(\frac{r}{c} \right)^2 - 1} - \arcsin \left(\frac{c}{r} \right) + \frac{\pi}{2} \right], \quad \text{for } c < r < a. \quad (43)$$

Examples for tangential contacts

Inserting the MDR transformed profiles into Eqs. (36) and (40), results in the relationships between radius c of the stick domain, ratio $F_x / (\mu F_N)$, and tangential displacement $u_x^{(0)}$. The results for the "classical profiles" of the sphere [4, 5], cone [23], as well as the power function profile are summarized in Table 4. The order of the rows corresponds to the order of the calculation steps.

Table 4 Solutions for the tangential contacts of simple profiles

3D profile $f(r)$	$r^2 / 2R$	$r \tan \theta$	$c_n r^n$
1D profile $g(x)$	x^2 / R	$\frac{\pi}{2} x \tan \theta$	$\kappa_n c_n x ^n$
$u_x^{(0)}$ according to (36)	$\mu \frac{E^*}{G^*} \left(d - \frac{c^2}{R} \right)$	$\mu \frac{E^*}{G^*} \left(d - \frac{\pi}{2} c \tan \theta \right)$	$\mu \frac{E^*}{G^*} \left(d - \kappa_n c_n c^n \right)$
$F_x / (\mu F_N)$ according to (40)	$1 - \left(\frac{c}{a} \right)^3$	$1 - \left(\frac{c}{a} \right)^2$	$1 - \left(\frac{c}{a} \right)^{n+1}$
Maximum static displacement according to (36)	$\mu d \left(E^* / G^* \right)$	$\mu d \left(E^* / G^* \right)$	$\mu d \left(E^* / G^* \right)$

6. CONCLUSIONS

In the present paper, we have limited ourselves to the essential rules and procedures of the method of dimensionality reduction. Evidence for the statements herein can be found in the works [1] and [15].

The possibilities of the MDR are much more expansive as presented in this composition. Further successful applications have been found for the rolling contact [24, 25], contacts with elastomers [26], contacts of rough surfaces [27, 28], elastomer friction [29], thermal effects in contacts [1], acoustic emission in rough contacts [31], and wear [32]. Interested readers are referred to the cited literature as well as the book [1]. In many cases, the MDR allows an analytical solution to the problem, as shown in this work.

However, it can also be easily implemented numerically and used for the investigation of systems with complex dynamic loadings [33].

Let us stress that the presented form of the MDR is only applicable to contacts with homogeneous elastic or viscoelastic half-spaces and it does not take into account size effects [34]. However, extensions to contacts with finite bodies or heterogeneous media are also possible [35]. The application of the MDR to rough contacts requires a separate paper.

REFERENCES

1. Popov, V.L., Hess, M., 2013, *Method of Dimensionality Reduction in Contact Mechanics and Friction*, Berlin Heidelberg: Springer-Verlag
2. Galin, L.A., 1961, *Contact Problems in the Theory of Elasticity*, North Carolina State College, USA
3. Sneddon, I.N., 1965, *The relation between load and penetration in the axisymmetric Boussinesq problem for a punch of arbitrary profile*, Int. J. Eng. Sci., 3(1), pp. 47-57.
4. Cattaneo, C., 1938, *Sul contatto di due corpi elastici: distribuzione locale degli sforzi*, Rendiconti dell'Accademia nazionale dei Lincei, 27, pp. 342-348, 434-436, 474-478.
5. Mindlin, R.D., 1949, *Compliance of elastic bodies in contact*, Journal of Applied Mechanics., 16, pp. 259-268.
6. Jaeger, J., 1995, *Axi-symmetric bodies of equal material in contact under torsion or shift*, Archive of Applied Mechanics, 65, pp. 478-487.
7. Ciavarella M., 1998, *Tangential Loading of General Three-Dimensional Contacts*. *Journal of Applied Mechanics*, 65, pp. 998-1003.
8. Galanov, B.A., 1993, *Development of analytical and numerical methods for study of models of materials*, Report for the project 7.06.00/001-92, 7.06.00/015-92. Kiev, Institute for Problems in Materials Science, (in Ukrainian)
9. Borodich, F.M., Galanov, B.A., 2004, *Molecular adhesive contact for indenters of nonideal shapes*, in: ICTAM04, Abstracts book and CD-Rom Proceedings, Warsaw, IPPT PAN
10. Borodich, F.M., 2008, *Hertz type contact problems for power-law shaped bodies*, in: Galin, L.A., Gladwell, G.M.L. (Eds.) "Contact Problems. The Legacy of L.A. Galin", Springer, 2008, pp. 261-292.
11. Yao, H., Gao, H., 2006, *Optimal shapes for adhesive binding between two elastic bodies*, Journal of colloid and interface science, 298(2), pp. 564-572.
12. Lee, E.H., 1955, *Stress analysis in viscoelastic bodies*, Quart. Appl. Math, 13, pp. 183-190.
13. Radok, J.R.M., 1957, *Viscoelastic stress analysis*, Quart. Appl. Math, 15, pp. 198-202.
14. Johnson, K.L., 1987, *Contact Mechanics*, Cambridge University Press
15. Hess, M., 2011, *Über die exakte Abbildung ausgewählter dreidimensionaler Kontakte auf Systeme mit niedrigerer räumlicher Dimension*, Cuvillier, Berlin, Germany
16. Hertz, H., 1882, *Über die Berührung fester elastischer Körper*, Journal für die reine und angewandte Mathematik, 92, pp. 156-171.
17. Boussinesq, V.J., 1885, *Application des Potentiels à l'étude de l'équilibre et du Mouvement des Solids Elastiques*, Gautier-Villar, Paris, France
18. Eijike, U.B.C.O., 1981, *The stress on an elastic half-space due to sectionally smooth-ended punch*, Journal of elasticity, 11(4), pp. 395-402.
19. Johnson, K.L., Kendall, K., Roberts A.D., 1971, *Surface energy and the contact of elastic solids*. Proceedings of the Royal Society of London, Series A, Mathematical and Physical Sciences, 324(1558), pp. 301-313.
20. Kendall, K., *The adhesion and surface energy of elastic solids*, Journal of Physics D: Applied Physics. 1971, 4, pp. 1186-1195.
21. Maugis, D., Barquins, M., 1981, *Adhesive contact of a conical punch on an elastic half-space*, Le Journal de Physique Lettres, 42(5), pp. 95-97.
22. Maugis, D., Barquins, M., 1983, *Adhesive contact of sectionally smooth-ended punches on elastic half-spaces: theory and experiment*, Journal of Physics D: Applied Physics, 16, pp. 1843-1874.
23. Truman, C.E., Sackfield, A., Hills, D.A., 1995, *Contact mechanics of wedge and cone indenters*, Int. J. Mech. Sci., 37, pp. 261-275.

24. Wetter, R., 2012, *Shakedown and induced microslip of an oscillating frictional contact*, Physical Mesomechanics, 2012, 15(5-6), pp. 293-299.
25. Wetter, R., Popov, V.L., 2014, *Shakedown limits for an oscillating, elastic rolling contact with Coulomb friction*. International Journal of Solids and Structures, 2014, 51(5), pp. 930-935.
26. Kürschner, S., Popov, V.L., 2013, *Penetration of self-affine fractal rough rigid bodies into a model elastomer having a linear viscous rheology*, Phys. Rev. E, 87, 042802.
27. Pohrt, R., Popov, V.L., Filippov, A.E., 2012, *Normal contact stiffness of elastic solids with fractal rough surfaces for one- and three-dimensional systems*, Phys. Rev. E, 86, 026710.
28. Pohrt, R., Popov, V.L., 2013, *Contact stiffness of randomly rough surfaces*. Sci. Rep. 3, 3293.
29. Li, Q., Popov, M., Dimaki, A., Filippov, A.E., Kürschner, S., Popov, V.L., 2013, *Friction Between a Viscoelastic Body and a Rigid Surface with Random Self-Affine Roughness*, Physical Review Letters, 111, 034301.
30. Popov, V.L., Voll, L., Li, Q., Chai, Y.S., Popov, M., 2014, *Generalized law of friction between elastomers and differently shaped rough bodies*, Sci. Rep. 2014, 4, 3750.
31. Popov, M., 2012, *Contact force resulting from rolling on self-affine fractal rough surface*, Physical Mesomechanics, 15(5-6), pp. 342-344.
32. Popov, V.L., 2014, *Analytic solution for the limiting shape of profiles due to fretting wear*, Sci. Rep., 4, 3749.
33. Teidelt, E., Willert, E., Filippov, A.E., Popov V.L., 2012, *Modeling of the dynamic contact in stick-slip micro-drives using the method of reduction of dimensionality*, Physical Mesomechanics, 15(5-6), pp. 287-292.
34. Argatov, I., 2010, *Frictionless and adhesive nanoindentation: Asymptotic modeling of size effects*, Mechanics of Materials, 42 (8), pp. 807-815.
35. Popov, V.L., 2014, *Method of dimensionality reduction in contact mechanics and tribology. Heterogeneous media*, Physical Mesomechanics, 17(1), pp. 50-57.

METODA DIMENZIONALNE REDUKCIJE U KONTAKTNOJ MEHANICI I TRIBOLOGIJI: UPUTSTVO ZA KORISNIKE I. AKSIJALNO-SIMETRIČNI KONTAKTI

Metoda dimenzionalne redukcije (MDR) predstavlja metodu za proračun i simulaciju kontakta elastičnih i viskoelastičnih tela. Suštinski se sastoji od dva jednostavna koraka: (a) zamene trodimenzionalnog kontinuuma jedinstveno definisanom jednodimenzionalnom linearno elastičnom ili viskoelastičnom podlogom (Winklerova podloga) i (b) transformacije trodimenzionalnog profila kontaktnih tela pomoću MDR-transformacije. Nakon izvršenja ova dva koraka, kontaktni problem se može smatrati rešenim. Za aksijalno-simetrične kontakte samo mali deo proračuna prevazilazi granice elementarnog računa i taj deo neće predstavljati prepreku za praktično orijentisanog inženjera. Kao alternativno rešenje, MDR se može primeniti i numerički, što je gotovo trivijalno zbog nezavisnosti elemenata podloge. I pored jednostavnosti, svi rezultati su egzaktni. Rad predstavlja kratak praktični vodič kroz MDR.

Ključne reči: *normalni kontakt, tangencijalni kontakt, adhezija, trenje, delimično klizanje, napon*